Research Square

Preprints are preliminary reports that have not undergone peer review.
They should not be considered conclusive, used to inform clinical practice,
or referenced by the media as validated information.

Investigation of the electrochemical sensor and DNA-binding properties of a novel picolinic acid-modified Anderson-based polyoxometalate hybrid compound

Eyüp Akgün

eakgun46@gmail.com

Kahramanmaraş Sütçü Imam University

Research Article

Keywords: POM-based hybrid, redox, electrochemical sensor, DNA binding

Posted Date: November 16th, 2026

DOI: https://doi.org/10.21203/rs.3.rs-11576204/v1

License: This work is licensed under a Creative Commons Attribution 4.0 International License.
Read Full License

Additional Declarations: No competing interests reported.

Investigation of the electrochemical sensor and DNA-binding properties of a novel picolinic acid-modified Anderson-based polyoxometalate hybrid compound

Eyüp Akgün

Kahramanmaraş Sütçü Imam University, Science Faculty, Chemistry Department, Kahramanmaraş, Türkiye

ABSTRACT

In this study, the organic-inorganic **AL2** hybrid compound ($Na_3[(C_6H_5NO_2)_3AlMo_6O_{24}H_6].2H_2O$) was synthesized in an acidic aqueous medium from the Anderson-type polyoxometalate compound $Na_3[AlMo_6O_{24}H_6]$ and picolinic acid/2-pyridinecarboxylic acid ($C_6H_5NO_2$). The compound was characterized using MALDI-TOF, FTIR, UV-Vis, and TGA/DTA spectroscopic techniques. Its electrochemical sensor performance toward Pb^{2+} ions and binding affinity with double-stranded fish sperm DNA (Fsds-DNA) were investigated. The binding parameters for Pb^{2+} ion interaction were calculated as $K_{sv} \approx 4x10^9\ M^{-1}$, LOD $\approx 4.5x10^9\ M^{-1}$, LOQ $\approx 1.5x10^9\ M^{-1}$, while the Fsds-DNA binding constant was determined to be $K_b = 3.14x10^6\ M^{-1}$.

Keywords: POM-based hybrid, redox, electrochemical sensor, DNA binding

Correspondence: Eyüp Akgün, **E-mail:** eakgun46@gmail.com, ORCID: 0009-0001-3421-7764

1. Introduction

In recent years, Anderson- and Keggin-based polyoxometalate (POM) hybrid compounds have yielded remarkable results in terms of cancer cell targeting and interaction with genetic material. Polyoxometalates are molecular oxide clusters capable of undergoing multi-electron transfer reactions. One of the most prominent features of POM hybrid compounds is their ability to release and accept a specific number of electrons without disrupting or altering their structural framework. Their capacity to bind to DNA and catalyze hydrolysis reactions, combined with tunable photophysical properties, makes them valuable tools in the development of novel therapeutic agents and advanced materials (Harrup and Hill 1996; Lİ and Wei 2021; Huang et al. 2016). Due to their high water solubility, pristine POMs can be unstable at the electrode surface; however, organic-inorganic hybridization enables POMs to form insoluble and stable films on electrode surfaces. Organic chromophores incorporated into the hybrid structure facilitate intermolecular charge transfer between the POM core and the organic ligand. This phenomenon enables optical sensing via fluorescence quenching or color changes in the presence of specific chemicals or ions. Investigations have been conducted regarding the production of POMs and certain POM-based hybrids exhibiting enhanced fluorescence and charge transfer properties for photonic and catalytic applications (Sullivan et al. 2017; Walsh et al. 2016). Owing to their high stability, they are employed in the precise electrochemical determination of hydrogen peroxide, dopamine, glucose, pH fluctuations, and heavy metal ions (Song et al. 2011; Veríssimo et al. 2022). The structural flexibility and biocompatibility of organic components, combined with the high redox activity, optical, and catalytic properties of the inorganic POM core, render these hybrids robust for both sensor technologies and DNA-targeted biomedical applications (Fu et al. 2015). They exhibit high catalytic currents and exceptionally low limits of detection (LOD) in electrochemical redox reactions (Zhang et al. 2022). Cyclic voltammetry (CV) serves as a powerful tool for examining the general electrochemical behavior of electrodes and is widely utilized in electrochemical sensor applications and DNA binding detection (Zhang et al. 2014; Gao et al. 2020). The coordination or interaction capability of POM-based organic-inorganic hybrid compounds with heavy metals in aqueous media can be precisely monitored via CV through current variations at the electrode surface. Similarly, when double-stranded DNA is incrementally added to a solution containing the POM hybrid, the electrochemical peak (CV signal) of the hybrid exhibits characterizable alterations. POM-based hybrid materials constructed from various organic ligands, such as triazolyl, carbazolyl, and pyridyl derivatives, have demonstrated exceptional catalytic and

sensing performances due to their tunable redox capabilities and low solubility. For instance, their electrocatalytic and sensing activities toward bromate, hydrogen peroxide, nitrite, and Cr(VI) have been comprehensively investigated. When polyoxometalates are functionalized with ligands containing amine, carboxyl, or phosphonate groups, they can be customized via covalent and hydrogen-bonding interactions to improve solubility, molecular recognition, biological activity, and electron transfer behavior. Their structural adaptability and tailorable functionality have driven extensive research into Anderson-type POM hybrids for applications across molecular electronics, photochemistry, magnetochemistry, and biomedicine. The aforementioned studies demonstrate that the functionalization of POMs can significantly enhance and improve their electrochemical performance, thereby increasing interest in their utilization as electrochemical sensors and capacitor electrode materials (Tong et al. 2024; Akgün et al. 2026).

In this study, the organic-inorganic **AL2** hybrid compound was synthesized from the inorganic Anderson-type polyoxometalate compound ($Na_3[AlMo_6O_{24}H_6]$) and the organic picolinic acid/2-pyridinecarboxylic acid ($C_6H_5NO_2$) ligand. The characterization of the **AL2** hybrid compound was performed using spectroscopic techniques including FTIR, UV-Vis, and MALDI-TOF mass spectrometry. The redox properties of **AL2** were investigated via cyclic voltammetry (CV), while its thermal behavior was examined using thermogravimetric analysis (TGA) and differential thermal analysis (DTA). Unlike our previous studies, which focused primarily on the DNA binding properties of synthesized hybrid compounds, this work evaluates both the DNA binding affinity and the electrochemical sensing performance toward Pb^{2+} ions utilizing the cyclic voltammetric method.

2. Experimental section

2.1 Materials and methods

All chemical substances used in this study and the equipments used to characterize the synthesized hybrid material are listed in the supplementary file. The synthesis of the Anderson POM-based hybrid material, data on its physical properties, and spectroscopic data are given in the supplementary file.

3. Results and discussion

3.1 Mass, FTIR, UV-vis spectral properties of the hybrid compound AL2

The proposed structure of the synthesized AL2 compound is presented in **Figure 1**. The MALDI-TOF technique was employed to acquire the mass spectrum of the organic-inorganic hybrid compound **AL2**. The mass spectrum of the **AL2** hybrid is presented in **Figure 2**, with the detailed mass spectrum in **Figure S1** and peak-ion assignments summarized in **Table 1**. The organic-inorganic hybrid compound **AL2** ($Na_3[(C_6H_5NO_2)_3AlMo_6O_{24}H_6].2H_2O$ consists of three moles of picolinic acid (L2), one mole of the Anderson-type aluminomolybdate anion ($[AlMo_6O_{24}H_6]^{3-}$), and two moles of crystal water. The Anderson aluminomolybdate anion located at the core of the hybrid architecture largely preserves its framework integrity even in the gas phase or undergoes controlled formation of lacunary derivatives via the loss of MoO_3 units. Peaks identified in the mass spectrum confirm the coordination of the organic ligand ($L=C_6H_5NO_2$) to the hybrid framework. Through multiple charge states (z = 1,2,3), ionization is observed to occur in the form of adducts balanced by metal cations (Na^+) and protons (H^+). Based on the mass spectrometric data, the **AL2** hybrid compound follows three primary fragmentation and ionization pathways. The first pathway comprises low-mass species: a mononuclear cationic adduct formed by a MoO_3 unit with sodium cations and the picolinate ligand at 314.046 m/z; intermediate fragments containing multiple ligands/protons resulting from the partial deconstruction of the Anderson framework at 359.036 m/z and 415.043 m/z; and triply-charged stable anionic adducts coordinated with four picolinate ligands via pentanuclear Anderson structures at 471.097 and 507.412 m/z. The second pathway involves intermediate-mass species: pentanuclear/hexanuclear transition adducts reaching a net 3^+ charge containing neutral MoO_3, four picolinate ligands, and six H^+ protons; doubly-charged primary coordination ions comprising the intact Anderson core structure ($[AlMo_6O_{24}H_6]^{3-}$) bearing three picolinate ligands balanced by sodium and protons at 683.507 m/z and 727.466 m/z; and highly coordinated doubly-charged structures formed by lacunary frameworks featuring high ligand numbers and MoO_3 losses. The third pathway encompasses high-mass species: dimeric adducts balanced by sodium cations following the loss of MoO_3 from a double Anderson framework at 1952.343 m/z; and clusters coordinated through combinations of multiple ligands and MoO_3 deconstruction of dimeric Anderson cores at 2184.978 m/z and 2417.248 m/z (Khan et al. 2021).

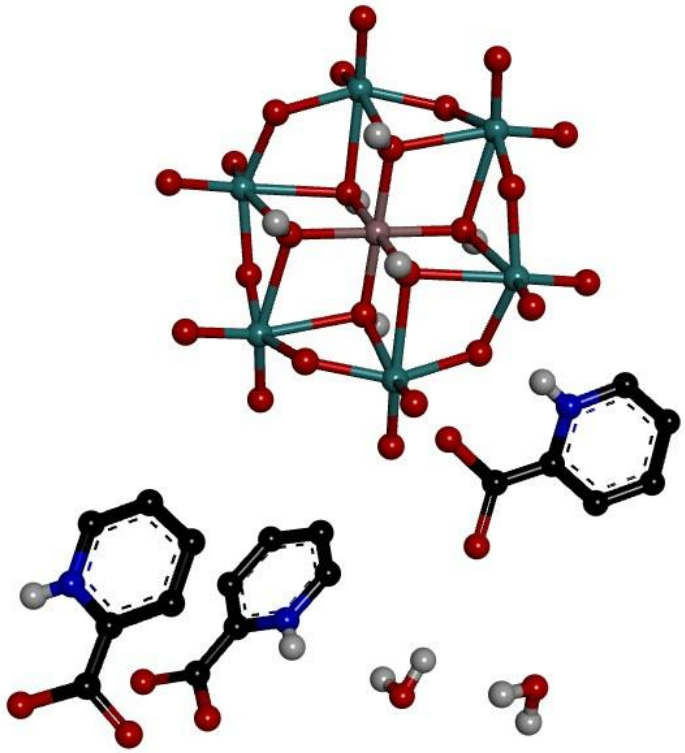


Figure 1: Proposed structure of the organic-inorganic hybrid compound AL2

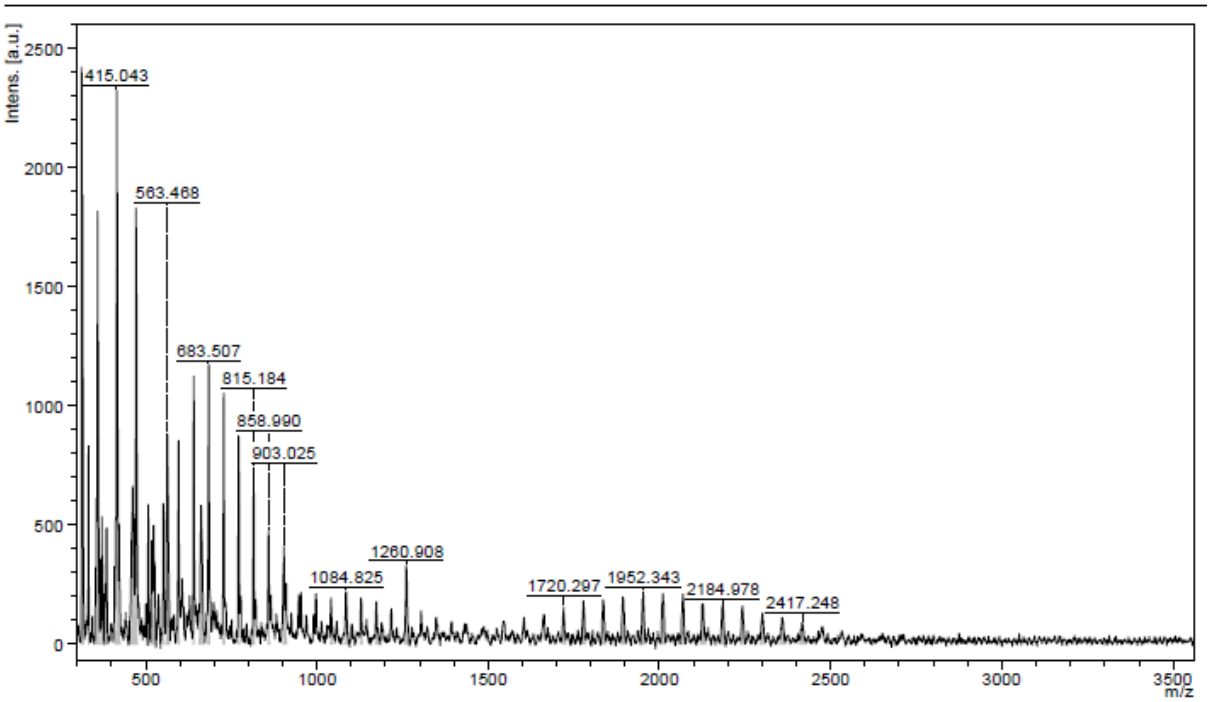


Figure 2: Mass spectrum of the organic-inorganic hybrid compound AL2

Table 1: Peak-ion assignment for the mass spectrum of the AL2 hybrid compound

Found m/z value	Proposed Fragments	Calculated Mass
314.046	$[(AlMo_6O_{24}H_6) + MoO_3 + 4L + 3H_2O + 6H]^{3+}$	314,038
359.036	$[(AlMo_4O_{18}H_4) + 2L + 3Na + 3H_2O + 3H]^{3+}$	359.036
415.043	$[(AlMo_5O_{21}H_6) + 3HL + Na + 2H]^{3+}$	415.373
471.097	$[(AlMo_5O_{21}H_6) + 4L + 4H_2O]^{3-}$	470.097
563.468	$[(AlMo_6O_{24}H_6) + L + 2Na + 3H - 2H_2O]^{2+}$	563.905
507.412	$[(AlMo_5O_{21}H_6) + 4L + 2H_2O]^{3-}$	507.063
595.591	$[(AlMo_5O_{21}H_6) - 2MoO_3 + 3L + Na + 5H_2O + 4H]^{2+}$	595.621
683.507	$[(AlMo_6O_{24}H_6) + 3L + Na - H_2O]^{2-}$	683.505
727.466	$[(AlMo_6O_{24}H_6) + 3L + 4Na + H]^{2+}$	727.504
771.277	$[(AlMo_5O_{21}H_6) - 2MoO_3 + 6L + Na + 4H_2O + 4H]^{2+}$	771.280
815.184	$[(AlMo_6O_{24}H_6) - MoO_3 + 5L + 4Na + H]^{2+}$	814.850
858.990	$[(AlMo_6O_{24}H_6)_2 + 4L + 5H_2O + 9H]^{3+}$	858.946
903.025	$[(AlMo_6O_{24}H_6) - 3MoO_3 + 2L + 5Na - H_2O - H]^{+}$	903.014
1260.908	$[AlMo_6O_{24}H_6) + 2L + H_2O + 4H]^{+}$	1260.950
1720.297	$[(AlMo_6O_{24}H_6) + 5L + 6H_2O + 4H]^{+}$	1720.255
1952.343	$[(AlMo_6O_{24}H_6)_2 - MoO_3 + 8Na - 4H_2O - H]^{+}$	1952.317
2184.978	$[(AlMo_6O_{24}H_6)_2 + L + 4Na - H_2O + 3H]^{+}$	2185.510
2417.248	$[(AlMo_6O_{24}H_6)_2 - 4MoO_3 + 6L + 7Na + 6H_2O]^{+}$	2417.310

The FTIR spectrum of the organic-inorganic hybrid compound **AL2** is illustrated in **Figure 3**. Evaluation of the FTIR spectrum reveals that the broad absorption band observed in the 3424-3300 cm^{-1} region originates from the crystal water molecules $\nu(H_2O)$ within the hybrid structure and the OH group of the carboxylic acid moiety in picolinic acid. Furthermore, this band's pronounced breadth is attributed to intramolecular N…H-O hydrogen bonding between the nitrogen atom on the pyridine ring and the hydrogen atom of the carboxyl group. The sharp, medium-intensity band observed at 3078 cm^{-1} arises from aromatic ν(C–H) stretching

vibrations of the pyridine ring and ν(N^+–H) stretching modes of the protonated pyridinium ring. The intense doublet bands at 1626 and 1601 cm^{-1} correspond to the asymmetric carboxylate stretching $\nu_{as}(COO^-)$ and ring ν(C=C)/ν(C=N) stretching vibrations. The carbonyl stretching peak ν(C=O) of free picolinic acid is shifted to a lower frequency at 1626 cm^{-1}, serving as evidence of carboxylate deprotonation or complexation via strong hydrogen bonding and coordination interactions. The band appearing at 1479 cm^{-1} is assigned to intra-ring ν(C=C)/ν(C=N) vibrations and ring bending modes of the pyridine ring. Bands observed at 1366 and 1297 cm^{-1} are attributed to the symmetric carboxylate stretching vibration $\nu_s(COO^-)$ and ν(C–O) stretching modes, respectively. The separation between the asymmetric and symmetric carboxylate stretching bands ($\Delta\nu$ = 1366-1626 = 260 cm^{-1}) indicates the ionic interaction character of the carboxylate group. Bands detected at 1150, 1094, and 1048 cm^{-1} are assigned to in-plane pyridine ring δ(C–H) bending and characteristic fingerprint vibrations of the picolinate ligand (Tella et al. 2017). The critical metal-oxygen (M–O) bands confirming the presence of the Anderson core appear in the 1000-450 cm^{-1} range. Specifically, bands at 855 and 825 cm^{-1} are assigned to terminal ν(M=O_t) stretching vibrations, whereas bands at 767 and 691 cm^{-1} correspond to molybdenum-oxygen-molybdenum bridging stretching modes ν(Mo–O_b–Mo) and ν(Mo–O_c–Mo) (Akgün et al. 2025).

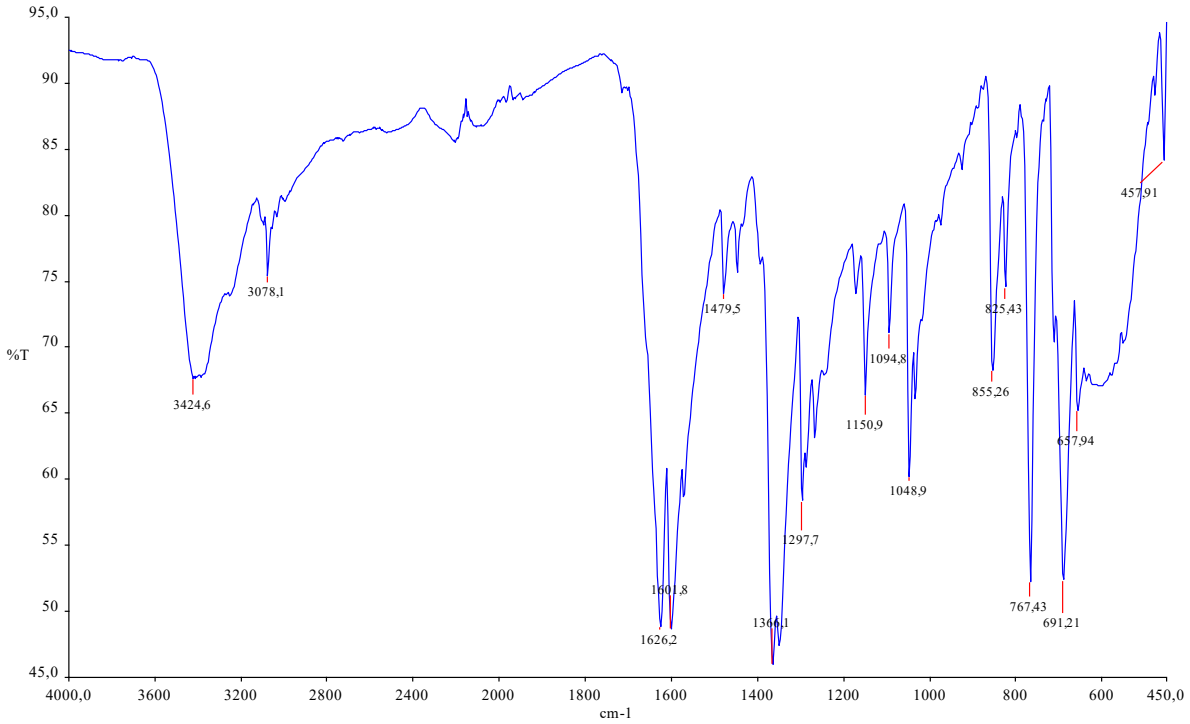


Figure 3: FTIR spectrum of the AL2 organic-inorganic hybrid compound

The electronic spectral properties of the Anderson-type polyoxometalate anion (A), picolinic acid (L2), and the hybrid compound **AL2** were examined in deionized water solution. The

spectrum of the Anderson-type polyoxometalate anion at a $1x10^{-4}$ M concentration is shown in **Figure 4**, that of picolinic acid $1x10^{-4}$ M in **Figure 5**, and that of the hybrid compound **AL2** (1 $1x10^{-5}$ M) in **Figure 6**. Picolinic acid, representing the organic moiety of the hybrid material, exhibits a sharp, intense absorption band at 273 nm and a weak band at 283 nm originating from n- π* transitions. The pristine Anderson polyoxometalate compound displays a broad absorption band at 272 nm due to n- π* transitions along with a shoulder-like absorption band at 280 nm. In contrast, the spectrum of the **AL2** hybrid compound reveals a remarkably broad absorption band spanning the 270-320 nm region, resulting from the overlap of n- π* transitions and charge-transfer transitions (LMCT/MLCT, O→Mo/Mo→O). While the principal absorption bands of the Anderson POM and L2 lie within the 271-272 nm range, the absorption band of the **AL2** hybrid shifts toward the 293-294 nm region. This prominent red-shift provides conclusive evidence of a strong electronic interaction between the picolinate ligand and the inorganic Anderson POM core.

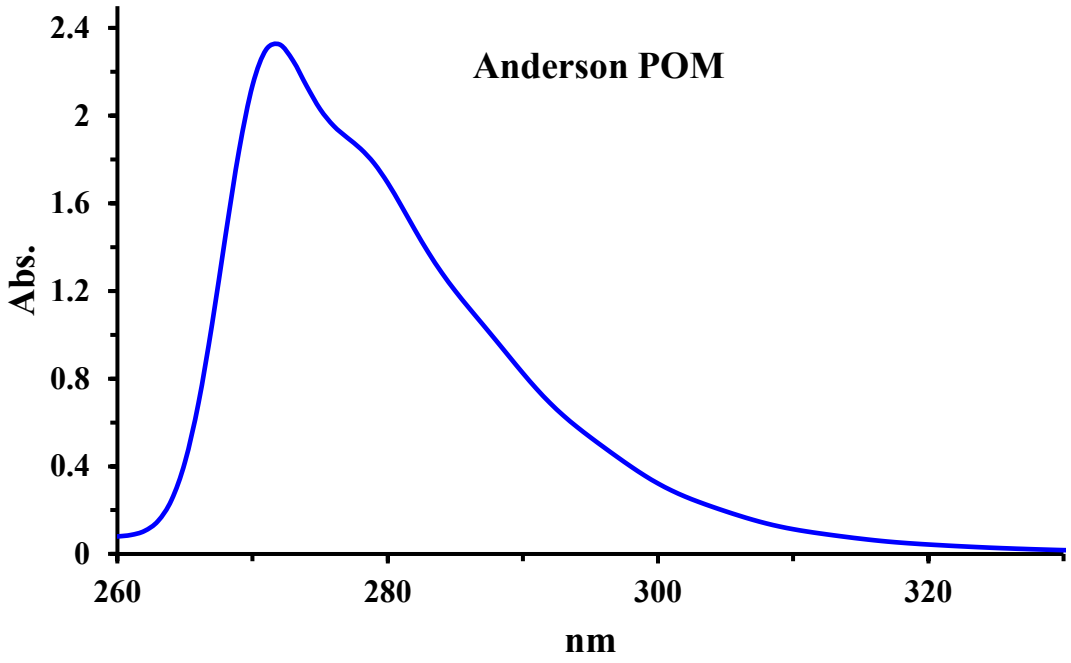


Figure 4: UV-vis spectrum of the Anderson polyoxometalate compound in a 10^{-4} M aqueous solution

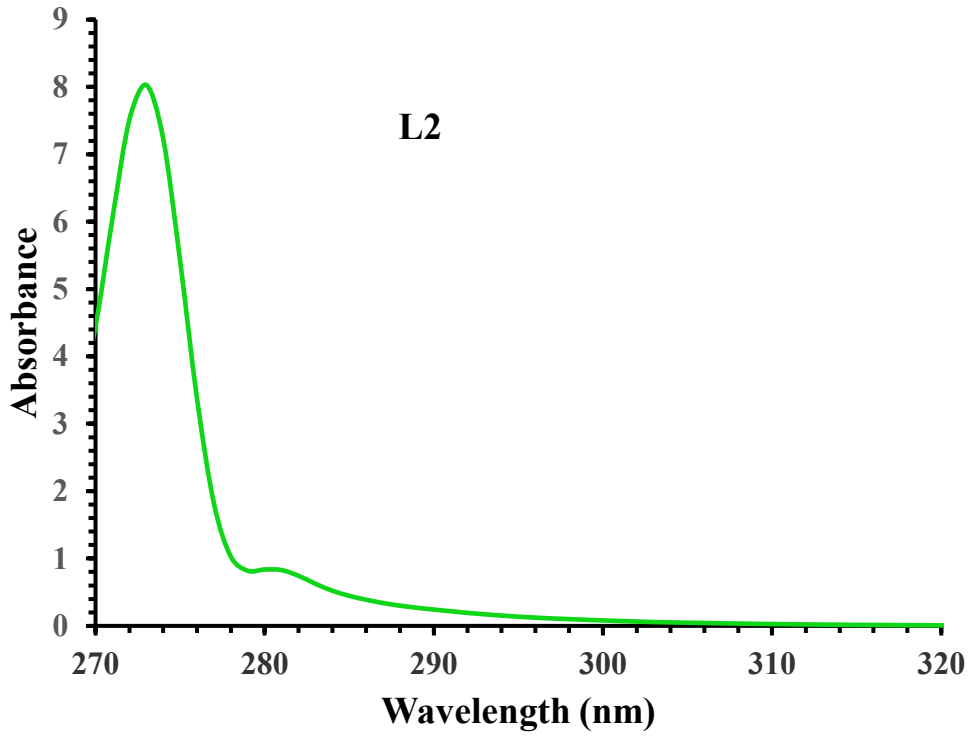


Figure 5: UV-vis spectrum of the L2 organic ligand in a 10^{-4} M aqueous solution

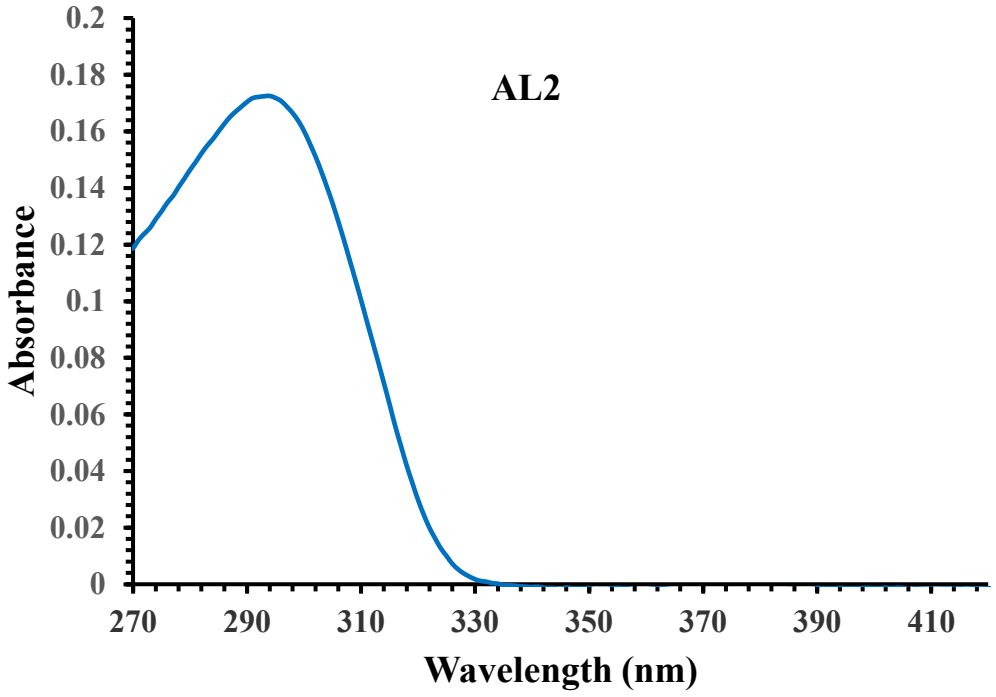


Figure 6: UV-vis spectrum of the AL2 hybrid compound in a 10^{-5} M aqueous solution

3.2 Thermal and electrochemical behaviors of the hybrid compound AL2

The thermal behavior of the organic-inorganic hybrid compound **AL2** was investigated within the temperature range of 30–980 °C under a N_2 atmosphere. The thermogravimetric analysis (TGA) curve of the **AL2** organic-inorganic hybrid compound is presented in **Figure 7**. According to the thermal profile, the thermal decomposition of the hybrid compound proceeds in four distinct stages. In the first decomposition stage (25–233 °C), a mass loss of %2.8 is observed, which corresponds to the elimination of crystallization water molecules from the lattice structure. During the second stage (233–435 °C), the mass percentage drops from 97.2% to 68.4%, yielding a net mass loss of 28.7%. This stage is attributed to the thermal dissociation and removal of the organic picolinic acid molecules from the hybrid framework. In the third stage (435–657 °C), mass loss occurs due to the breakdown of the Anderson core within the hybrid compound. The condensation and elimination of hydroxyl groups (–OH) as H_2O from the Anderson anion ($[AlMo_6O_{24}H_6]^{3-}$) result in the formation of Al_2O_3 and MoO_3 metal oxides. In this stage, the mass decreases from 68.4% to 46.8%, with a net mass loss of 21.6%. In the fourth stage, at temperatures above 658 °C, the TGA curve exhibits a gradual decline owing to the sublimation and volatilization losses of MoO_3. The TGA analytical data confirm that the hydration number of crystallization water in the organic-inorganic **AL2** hybrid is 2 mol. Overall, the mass spectrometric, FTIR, and TGA spectra collectively corroborate the proposed structure comprising the inorganic Anderson polyoxometalate core, the organic picolinic acid ligand, and lattice water molecules (Akgün et al. 2025).

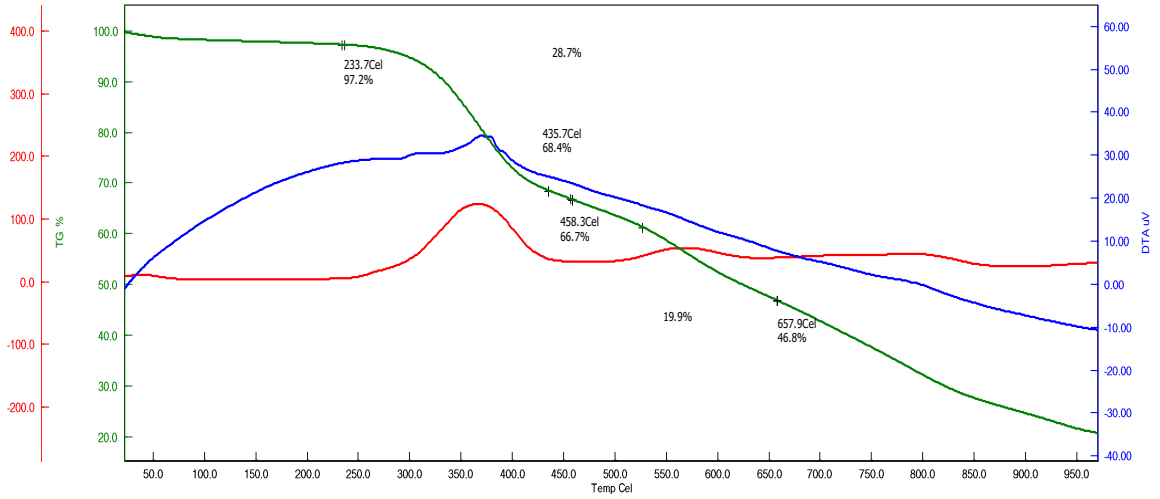


Figure 7: Thermal curves of the organic-inorganic hybrid compound AL2

Cyclic voltammetry (CV) measurements were performed to investigate the redox properties of the **AL2** hybrid compound. Cyclic voltammetric measurements were carried out at room

temperature in an undivided cell equipped with a platinum counter electrode and an Ag^{+}/AgCl reference electrode. Based on the CV analysis of a $1x10^{-4}$ M Tris-buffered solution of **AL2** recorded within the potential window of -2–2 V at scan rates ranging from 100-1000 mV/s, the cyclic voltammograms presented in **Figure 8** were obtained. The cyclic voltammograms of **AL2** reveal two reduction and two oxidation potentials spanning an anodic and cathodic peak potential (E_{pa} ve E_{pc}) range of -1,36 ile (+)0,29 V. Notably, only a single oxidation potential is observed at the scan rate of 100 mV/s. The E_{pa} values range from -0,32 to 0,29 V, whereas the E_{pc} values lie between -1,36 and (-)0,36 V. The redox processes are irreversible across all tested scan rates. As the scan rates increase (from the black curve to the red curve), a regular and linear enhancement in both cathodic and anodic peak current intensities is observed. Furthermore, increasing scan rates induce a positive shift in cathodic peak potentials and a negative shift in anodic peak potentials. The polygonal and expanded current responses demonstrate that the hybrid framework comprising the inorganic Anderson core and organic picolinate ligands possesses high electrochemical stability over a wide potential window (-2–2 V). The attainment of current values reaching -90–(+)160 µA at high scan rates provides evidence that the electroactive surface area and electronic conductivity of the material are highly favorable for sensor applications.

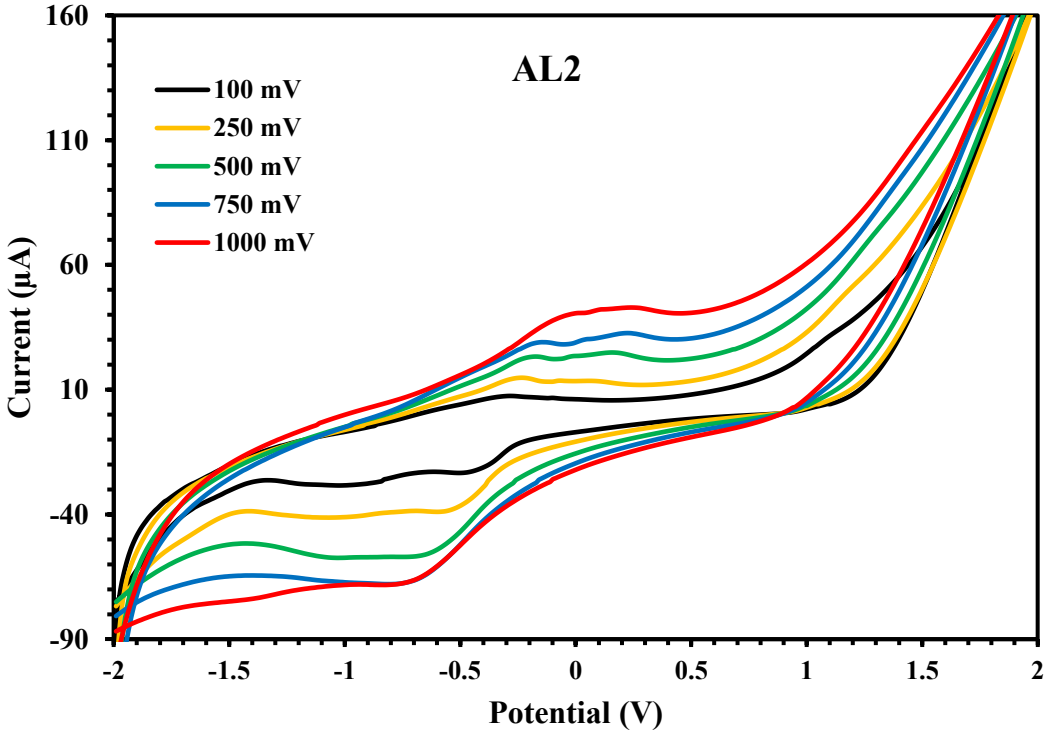


Figure 8: CV curves of the AL2 hybrid compound in a $1x10^{-4}$ M Tris-buffered solution, recorded at scan rates ranging from 100 to 1000 mV/s

3.3 Sensor studies of the AL2 hybrid compound

UV-Vis, photoluminescence, and cyclic voltammetry studies were performed to evaluate the sensor performance, metal selectivity, and optical response mechanism of the **AL2** hybrid compound. In the UV-Vis study, a $1x10^{-5}$ M aqueous solution of the **AL2** hybrid compound was employed. Metal ion solutions (K^{+}, Mg^{2+}, Al^{3+}, Fe^{3+}, Cu^{2+}, Cr^{3+}, Co^{2+}, Ni^{2+}, Zn^{2+}, Mn^{2+}, Cd^{2+}, Pb^{2+} and Hg^{2+}) were prepared at $1x10^{-5}$ M in methanol using their chloride or nitrate salts. The AL2:M^{n+} (1:1) UV-Vis spectrum (**Figure 9**) was obtained upon the addition of metal ions to the $1x10^{-5}$ M aqueous solution of **AL2**. Examination of the UV-Vis spectra reveals that the addition of most metal ions results in a decrease in absorbance values (hypochromic effect) or comparable band positions relative to pristine **AL2**. Conversely, the blue curve representing the AL2-Pb^{2+} interaction upon lead addition diverges markedly from all other metal ions and free **AL2** by exhibiting a hyperchromic effect. Furthermore, the emergence of a new absorbance band at 350 nm upon Pb^{2+} addition indicates a distinct interaction mode compared to other metal ions. This pronounced spectral alteration serves as optical evidence that the **AL2** hybrid compound possesses superior affinity and selectivity toward Pb^{2+} ions in aqueous media. To corroborate this property, photoluminescence and cyclic voltammetry investigations were conducted.

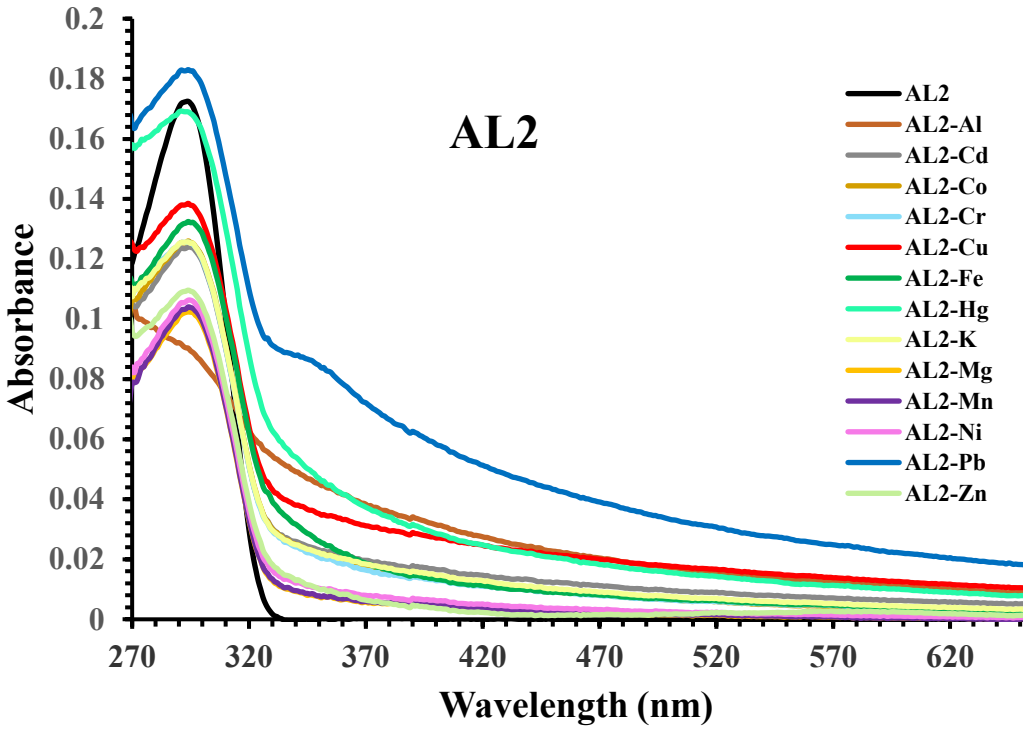


Figure 9: UV-vis spectrum of the AL2 hybrid compound in a 10^{-5} M aqueous solution upon the addition of a metal ion (AL2:M^{n+}, 1:1 ratio)

In the photoluminescence study, a $1x10^{-5}$ M aqueous solution of the **AL2** hybrid compound and a $1x10^{-8}$ M Pb^{2+} ion solution prepared in methanol were utilized. The emission spectrum (**Figure 10**) was acquired upon the incremental addition (10-100µL) of the $1x10^{-8}$ M Pb^{2+} ion solution to the $1x10^{-5}$ M aqueous **AL2** solution under excitation at 325 nm. Analysis of the emission spectrum indicates that when the free **AL2** solution is excited at 325 nm, it exhibits a high-intensity (848 a.u) fluorescence emission band at 341 nm. Upon the progressive addition of Pb^{2+} ions to the medium, a regular decrease in emission intensity (quenching effect) is observed. Following the addition of 100 µL of Pb^{2+}, the fluorescence intensity drops by more than half (405 a.u). This behavior demonstrates that the **AL2** hybrid compound can detect trace amounts of Pb^{2+} ions in aqueous media with high sensitivity (fluorescence turn-off sensor behavior). The Stern-Volmer plot derived from the emission spectra upon incremental Pb^{2+} additions is presented in **Figure 11**. The calibration equation yielded a correlation coefficient of $R^2 = 0.948$, while the binding constant, limit of detection (LOD), and limit of quantification (LOQ) were calculated as $K_{sv} \approx 4x10^{9}$ M^{-1}, LOD $\approx 4.5x10^{9}$ M^{-1}, and LOQ $\approx 1.5x10^{9}$ M^{-1}, respectively. The high K_{sv} value further confirms that the **AL2** hybrid compound possesses a strong binding and quenching affinity toward lead ions. Given that the detection limit of **AL2** for Pb^{2+} ions in aqueous media lies in the nanomolar range, it exhibits outstanding sensing performance for environmental water analysis.

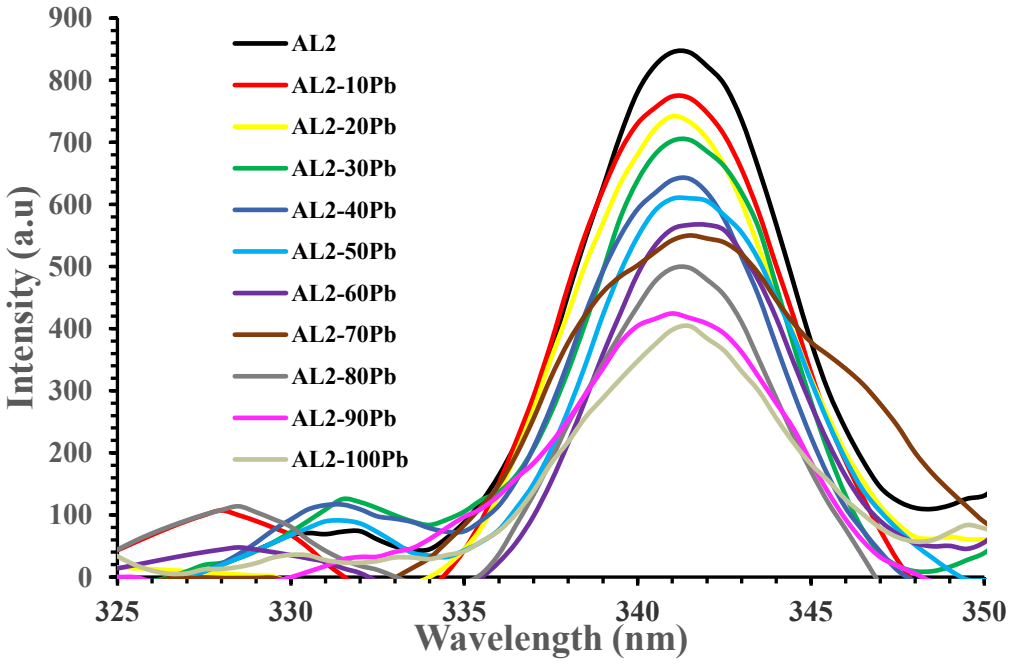


Figure 10: Emission spectrum resulting from the incremental addition of Pb^{2+} to the AL2 hybrid compound

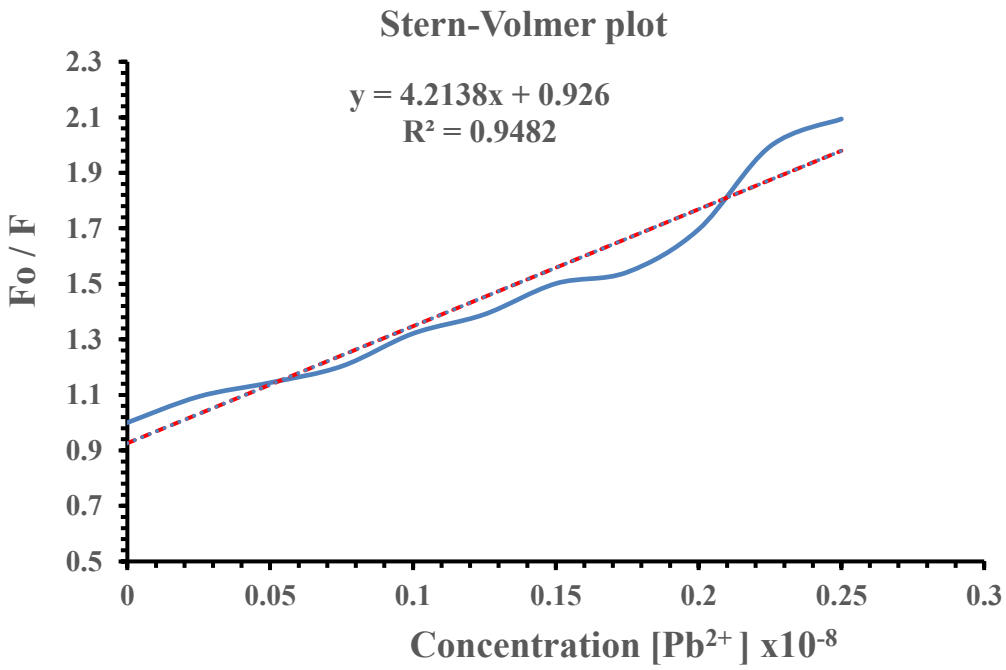


Figure 11: Stern-Volmer plot derived from the emission spectra obtained upon the incremental addition of Pb^{2+} to the AL2 hybrid compound

The electrochemical kinetic data of the **AL2** hybrid are summarized in **Table 2**, and the Randles–Sevcik plot is displayed in **Figure 12**. According to the theory, a slope approaching 0.5 indicates a diffusion-controlled electrochemical process (where electroactive species are transported from the bulk solution to the electrode via mass transfer), whereas a slope close to 1.0 signifies an adsorption-controlled process (indicating surface-bound electroactive species). Intermediate slope values between 0.5 and 1.0 point to a combined mechanism involving both processes. The slope value of 0.84 in the Randles–Sevcik plot of the **AL2** hybrid proves that adsorption-controlled kinetics is predominant, accompanied by a contributory diffusion component. This strong electroactive adsorption tendency at the electrode interface is likely the primary factor underlying the high sensitivity demonstrated by the **AL2** hybrid material in electrochemical sensor applications and surface-based analyte detection.

Table 2: Electrochemical kinetic data for the AL2 compound: Log(Ipa) vs. Log(ν)

Tarama Hızı (mV/s)	**Log(ν) (mV/s)**	**Anodik pik akımı (µA)**	**Log(*Ipa*) (µA)**
100	2.000	6	0.778

250	2.398	13	1.114
500	2.699	24	1.380
750	2.875	32	1.505
1000	3.000	42	1.623

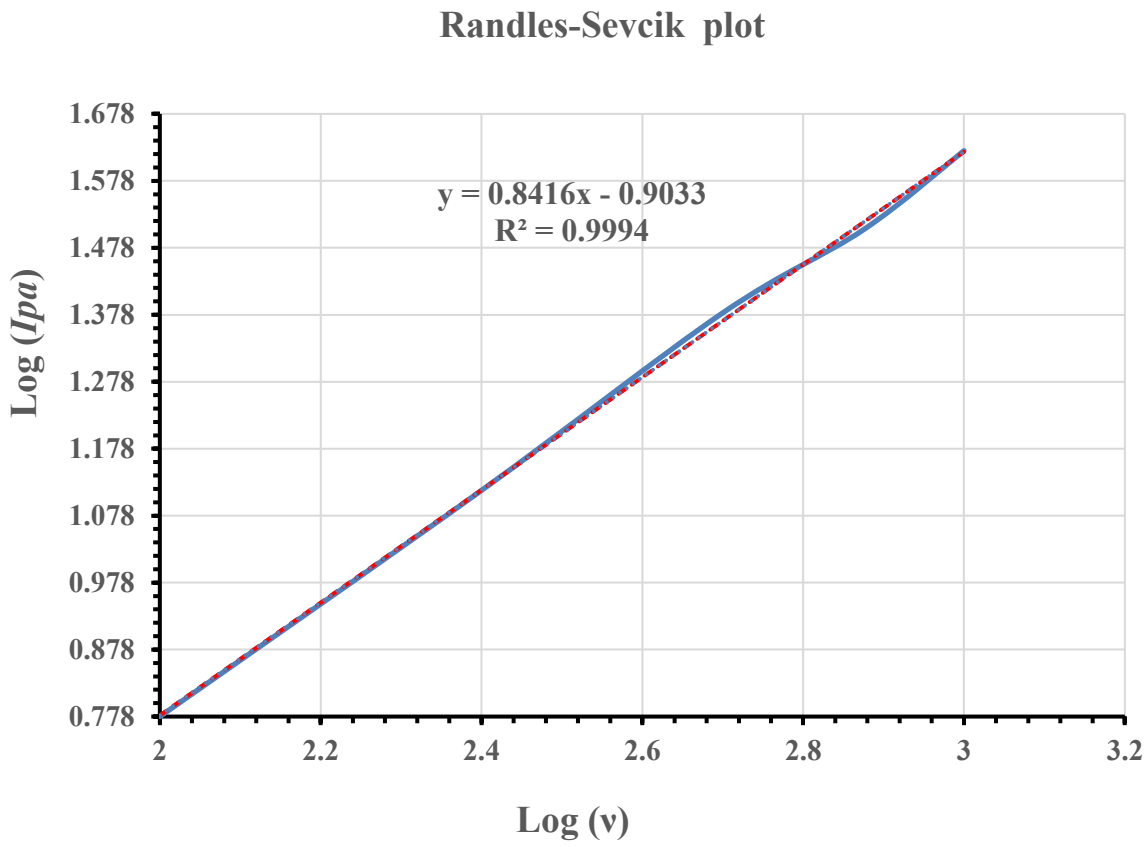
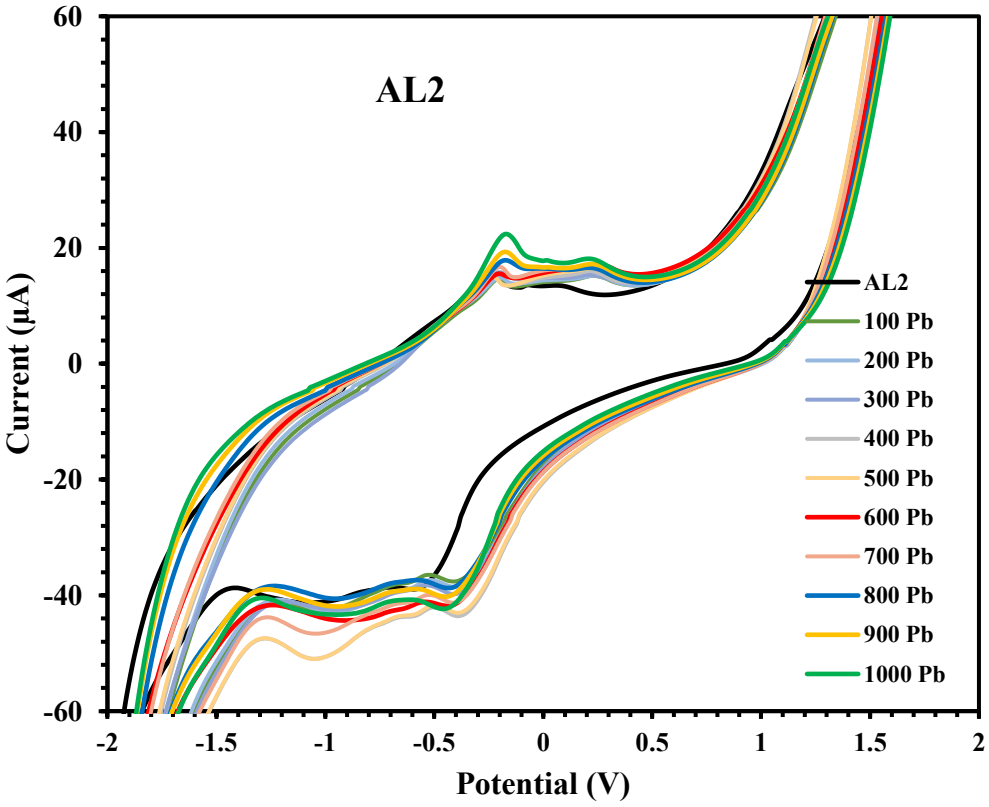


Figure 12: Randles-Sevcik plot for the AL2 compound

Electrochemical studies were performed using a $1x10^{-4}$ M aqueous solution of the **AL2** hybrid compound and a $1x10^{-8}$ M Pb^{2+} ion solution prepared in methanol. Measurements were recorded within a potential window of -2 – (+2) at a constant scan rate of 250 mV/s upon the incremental addition (100-1000 µL) of the $1x10^{-8}$ M Pb^{2+} solution to the $1x10^{-4}$ M aqueous **AL2** solution (**Figure 13**). The *Ipa*–[Pb^{2+}] data extracted from this plot at a potential of -0.17 V are presented in **Table 3**. As Pb^{2+} ions are introduced into the solution, the peak current intensity of the first anodic peak located at approximately -0.17 V increases markedly from 14.5 µA to 22.4 µA. A similar enhancement is observed in the current intensity of the second anodic peak centered around 0.24 V. This progressive current enhancement represents a hyperchromic anodic response of the **AL2** hybrid compound toward Pb^{2+} ions. This prominent "turn-on" type anodic

current behavior confirms the formation of an electrochemically active AL2-Pb^{2+} interaction at the electrode interface. Consequently, the ability of **AL2** to detect Pb^{2+} ions at nanomolar levels (10–100 nM) validates its superior sensitivity and quantitative electrochemical detection performance.



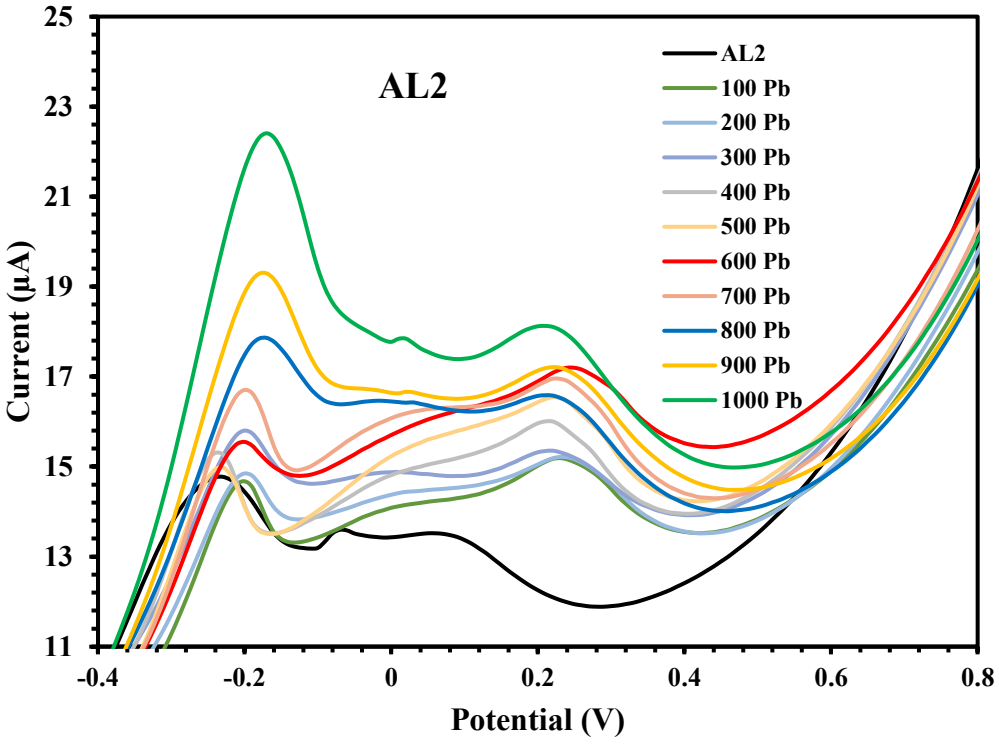


Figure 13: CV curves obtained by the incremental addition (100–1000 µL) of 1×10^{-8} M Pb^{2+} ions to a 1×10^{-4} M aqueous solution of the AL2 hybrid compound, at a scan rate of 250 mV/s

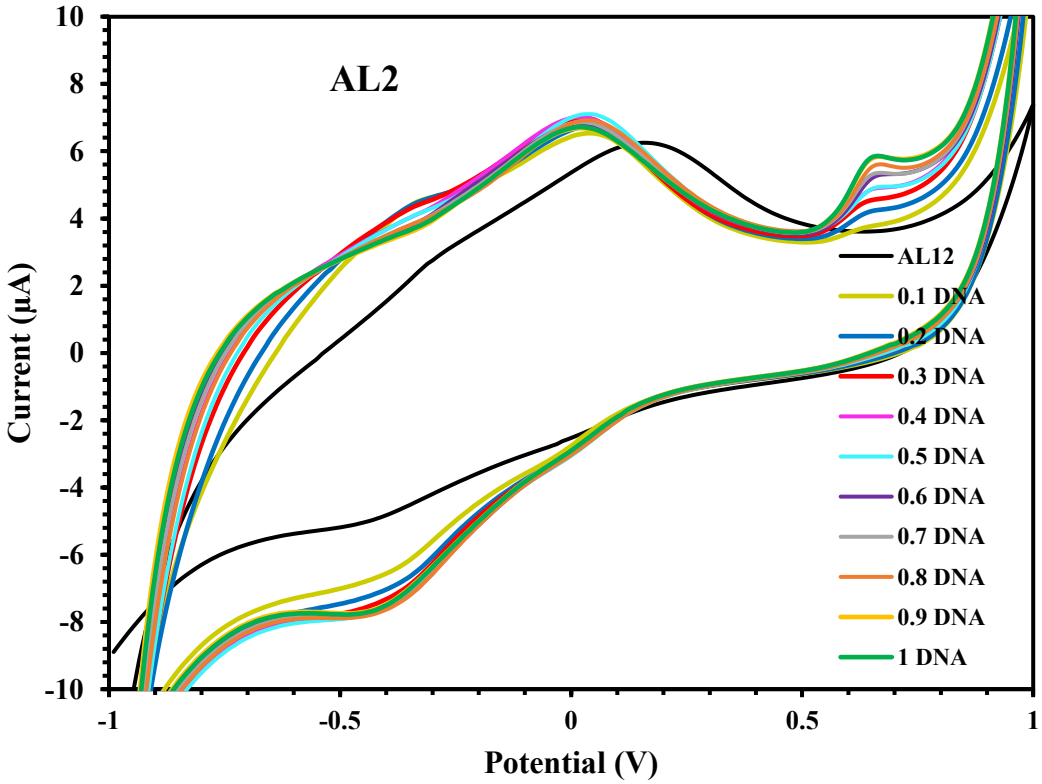
Table 3: Electrochemical data (*Ipa vs. [Pb^{2+}]*) for compound AL2 at a scan rate of 250 mV/s

Ipa (µA) (-0.17 V)	14.5	14.8	15	15.4	15.5	15.7	16.7	17.8	19.3	22.4
[Pb^{2+}] (nM) konsantrasyonu	10	20	30	40	50	60	70	80	90	100

3.4 DNA binding studies of the AL2 hybrid compound

The interaction of the **AL2** hybrid compound with double-stranded fish sperm DNA (Fsds-DNA) was investigated in a Tris-buffered solution using cyclic voltammetry. The cyclic voltammograms obtained upon the incremental addition (0.1–1 mL) of a $1x10^{6-}$ M DNA solution to a 10 mL aqueous solution of **AL2** $1x10^{-5}$ M at a scan rate of 200 mV/s are presented in **Figure 14**. Upon the progressive addition of DNA to the medium, distinct and systematic alterations were observed in the cyclic voltammograms within the potential range of -0.3–(+)0.9 V. The addition of DNA induced notable shifts in both anodic and cathodic peak potentials. A prominent new anodic peak emerged at approximately 0.65 V, and as the DNA addition increased from 0.1 mL to 1 mL, the peak current intensity exhibited a regular increase from 3.6

µA to 5.85 µA. These observed electrochemical responses confirm a strong binding affinity and efficient electronic interaction between **AL2** and DNA. The Benesi-Hildebrand data table, prepared using data extracted from the CV titration spectra (specifically the anodic peak current enhancements at the 0.65 V potential), is given in **Table 4**, and the corresponding binding plot is displayed in **Figure 15**. The correlation coefficient was determined as $R^2 = 0.9862$, and the binding constant was calculated as $K_b = 3.14 \times 10^6$ M^{-1}. These results corroborate that the **AL2** hybrid compound forms a stable supramolecular interaction with DNA on the order of 10^6 M^{-1} and possesses a strong affinity for nucleic acid detection. Polyoxometalate hybrid compounds modified with organic ligands generally tend to bind via the minor groove of DNA (Akgün et al. 2025).



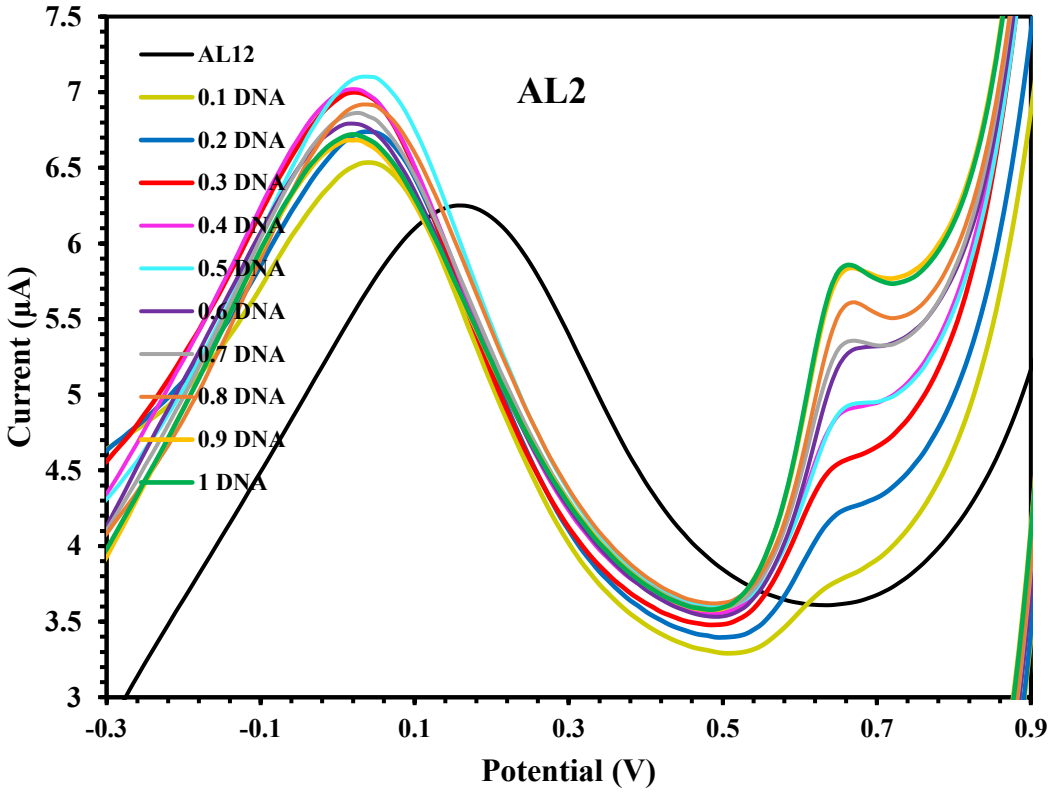


Figure 14: CV curves obtained by the incremental addition of $1x10^{-6}$ M Tris-buffered DNA to a $1x10^{-5}$ M aqueous solution of the AL2 hybrid compound, at a scan rate of 200 mV/s

Table 4: Benesi-Hildebrand data plot for the AL2 hybrid compound

Eklenen DNA hacmi (mL)	**Hücre içi [DNA]**	**Anodik pik akımı (μA)**	**$\Delta I=I-I_0$ (μA)**	**1/[DNA] M^{-1}**	**$1/I-I_0$ (μA^{-1})**
0.2	$1.96x10^{-8}$	4.21	0.61	$5.10x10^{7}$	1.639
0.3	$2.91x10^{-8}$	4.54	0.94	$3.43x10^{7}$	1.064
0.4	$3.85x10^{-8}$	4.92	1.32	$2.60x10^{7}$	0.758
0.5	$4.76x10^{-8}$	4.95	1.35	$2.10x10^{7}$	0.741
0.6	$5.66x10^{-8}$	5.29	1.69	$1.77x10^{7}$	0.592
0.7	$6.54x10^{-8}$	5.35	1.75	$1.53x10^{7}$	0.571
0.8	$7.41x10^{-8}$	5.61	2.01	$1.35x10^{7}$	0.498
0.9	$8.26x10^{-8}$	5.81	2.21	$1.21x10^{7}$	0.452
1.0	$9.09x10^{-8}$	5.85	2.25	$1.10x10^{7}$	0.444

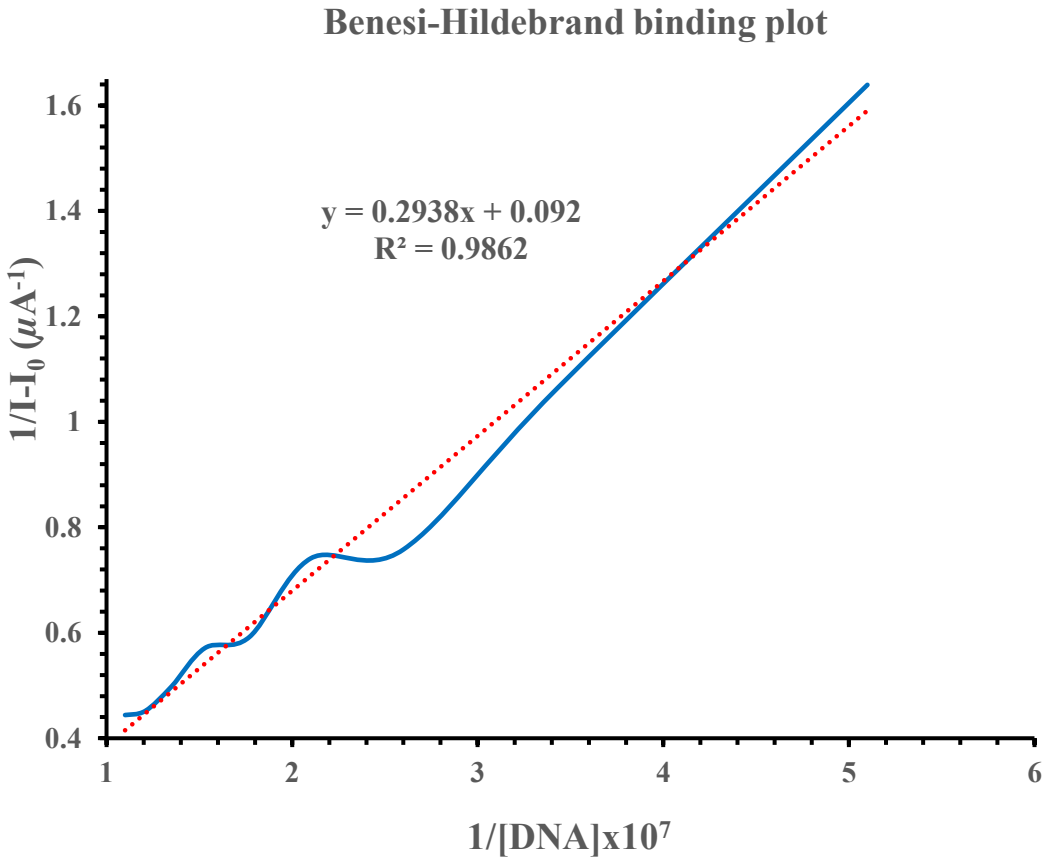


Figure 15: Benesi-Hildebrand binding plot for the AL2 hybrid compound

4. Conclusions

The organic-inorganic hybrid compound **AL2** was successfully prepared using the Anderson polyoxometalate ($Na_3[(AlMo_6O_{24}H_6].2H_2O$) and picolinic acid ($C_6H_5NO_2$) precursors and characterized via MALDI-TOF, FTIR, and UV-Vis spectroscopic techniques. Its thermal stability was evaluated within the temperature range of 30–980 °C under a N_2 atmosphere using TGA and DTA analyses. The analytical findings exhibit strong consistency with Anderson polyoxometalate-based hybrid compounds previously synthesized and characterized by single-crystal X-ray diffraction in our group. Cyclic voltammetric measurements of **AL2** revealed two reduction and two oxidation potentials, with anodic and cathodic peak potentials (E_{pa} and E_{pc}) spanning the range of -1,36 ile (+)0,29 V. These results demonstrate that the **AL2** hybrid compound possesses remarkable electrochemical stability across a wide potential window (-2–2 V). The attainment of current values reaching -90–(+)160 µA at high scan rates provides evidence that the electroactive surface area and electronic conductivity of the material are highly favorable for sensor applications. The sensing performance of **AL2** toward Pb^{2+} ions

was investigated through UV-Vis absorption, photoluminescence, and cyclic voltammetry. Based on the Stern-Volmer analysis of the photoluminescence data, the calibration correlation coefficient, binding constant, limit of detection (LOD), and limit of quantification (LOQ) were determined as R^2 = 0.948, $K_{sv} \approx 4x10^9$ M^{-1}, LOD ≈ $4.5x10^9$ M^{-1}, and LOQ ≈ $1.5x10^9$ M^{-1}, respectively. Furthermore, the DNA binding affinity was examined using cyclic voltammetry, yielding a correlation coefficient of R^2 = 0.9862 and a Benesi-Hildebrand binding constant of $K_b = 3.14x10^6$ M^{-1}. Overall, this study highlights the promising potential of functionalizing Anderson-type POMs with picolinic acid for the development of advanced electrochemical sensor hybrid materials and biomedical applications.

Acknowledgments

The author expresses her thanks to Prof. Dr. Mehmet Tümer.

CRediT authorship contribution statement

Eyüp Akgün: Writing – review & editing, Writing – original draft, Methodology, Investigation, Formal analysis, Conceptualization.

Declaration of competing interest

The author declare that they have no known competing financial interests or personal relationships that could have appeared to influence the work reported in this paper.

References

Akgün E, Deligönül N, Comertpay S, Ballı JN, Tümer M (2026) Pyridine-based Anderson-type polyoxometalate hybrid: Synthesis, structural elucidation, and electrochemical and biological properties. Journal of Molecular Structure 1360 145522. https://doi.org/10.1016/j.molstruc.2026.145522

Akgün E, Deligönül N, Mısır BA, Tümer M, Comertpay S, Güngör Ö, Köse M, Akkaya OB (2025) Keggin POM-based hybrids decorated with aminopyridines. Determination of their molecular structure, electrochemical behaviors, antimicrobial and anticancer activities. Journal of Molecular Structure 1347 143278. https://doi.org/10.1016/j.molstruc.2025.143278

Akgün E, Mısır BA, Comertpay S, Köse M, Tümer M (2025) Keggin and Anderson POM-based hybrids modified by 4-pyridinepropanol: Synthesis, crystal structures, photophysical and DNA binding properties. Polyhedron 269 117418. https://doi.org/10.1016/j.poly.2025.117418

Akgün E, Mısır BA, Köse M, Tümer M (2025) Synthesis, structural characterization, electrochemical, photophysical and DNA binding properties of two Anderson POM-based hybrids. Journal of Molecular Structure 1319 139560. https://doi.org/10.1016/j.molstruc.2024.139560

Fu L, Gao H, Yan M, Li S, Li X, Dai ZH, and Liu S (2015) Polyoxometalate-Based Organic–Inorganic Hybrids as Antitumor Drugs. Small 11 24. https://doi.org/10.1002/smll.201500232

Gao J, Yang T, Wang X, He Q, He P, Jia L, Du L, Deng H, Zhang H, Jia B, He X, Tang B (2020) Spherical phosphomolybdic acid immobilized on graphene oxide nanosheets as an efficient electrochemical sensor for detection of diphenylamine. Microchemical Journal 158 105158. https://doi.org/10.1016/j.microc.2020.105158

Harrup MK, Hill CL (1996) Thermal multi-electron transfer catalysis by polyoxometalates. Application to the practical problem of sustained, selective oxidation of hydrogen sulfide to sulfur. Journal of Molecular Catalysis A: Chemical 106 57-66.

Huang Y, Zhang J, Hao J, Wei Y (2016) A general and highly regioselective synthesis approach to multifunctionalized organoimido derivatives of Polyoxometalates. Scientific Reports 6 24759. https://doi.org/10.1038/srep24759

Khan MA, Shakoor Z, Akhtar T, Sajid M, Asif HM (2021) Exploration on χ-Anderson type Polyoxometalates based hybrids towards photovoltaic response in solar cell. Inorganic Chemistry Communications 133 108875. https://doi.org/10.1016/j.inoche.2021.108875

Li Q and Wei Y (2021) Synthesis of organic-inorganic hybrid compounds and their self-assembled behavior in different solvents. Chem. Commun. 57 3865–3868. https://doi.org/10.1039/d1cc00563d

Song YF, Long DL, Rıtchıe C, Cronın L (2011) Nanoscale Polyoxometalate-Based Inorganic/Organic Hybrids. The Chemical Record 11 158–171. https://doi.org/10.1002/tcr.201100002

Sullivan KP, Neiwert WA, Zeng H, Mehta AK, Yin Q, Hillesheim DA, Vivek S, Yin P, Collins-Wildman DL, Weeks ER, Liu T and Hill CL (2017) Polyoxometalate-based gelating networks for entrapment and catalytic decontamination. Chem. Commun. https://doi.org/10.1039/c7cc05657e

Tella AC, Oladipo AC, Adeyemi OG, Oluwafemi OS, Oguntoye SO, Alimi LO, Ajayi JT, Degni SK (2017) Solid state synthesis, spectroscopic and X-ray studies of metal complexes of 2-picolinic acid and vapochromic behavior of $[Co(Pic)_2(H_2O)_2].2H_2O$. Solid State Sciences 68 1-9. http://dx.doi.org/10.1016/j.solidstatesciences.2017.03.017

Tong N, Wang X, Zhao XY, Zhang W, Zhu YS (2024) Construction of anderson–type polyoxometalate–based complexes involving in situ ligand transformation with capacitive and electrochemical sensing performances. Inorganica Chimica Acta 562 121901. https://doi.org/10.1016/j.ica.2023.121901

Veríssimo MIS, Evtuguin DV and Gomes MTSR (2022) Polyoxometalate Functionalized Sensor: A Review. Frontiers in Chemistry 10 840657. https://doi.org/10.3389/fchem.2022.840657

Walsh JJ, Bond AM, Forster RJ, Keyes TE (2016) Hybrid polyoxometalate materials for photo(electro-) chemical applications. Coordination Chemistry Reviews 306 217–234. https://dx.doi.org/10.1016/j.ccr.2015.06.016

Zhang S, He P, Lei W, Zhang G (2014) Novel attapulgite/polyaniline/phosphomolybdic acid-based modified electrode for the electrochemical determination of iodate. Journal of Electroanalytical Chemistry 724 29–35. http://dx.doi.org/10.1016/j.jelechem.2014.04.011

Zhang Y, Wang X, Wang Y, Xu N and Wang XL (2022) Anderson-type polyoxometalate-based sandwich complexes bearing a new “V”-like bis-imidazole-bis-amide ligand as electrochemical sensors and catalysts for sulfide oxidation. Polyoxometalates 1 9140004. https://doi.org/10.26599/POM.2022.9140004

Supplementary Files

This is a list of supplementary files associated with this preprint. Click to download.

- Supplementaryfile.docx